APL MATERIALS **5**, 035301 (2017)

Perspectives: Nanofibers and nanowires for disordered photonics

Dario Pisignano,[1,2,a] Luana Persano,[2,b] and Andrea Camposeo[2,c]
[1]*Dipartimento di Matematica e Fisica "Ennio De Giorgi," Università del Salento, via Arnesano, I-73100 Lecce, Italy*
[2]*NEST, Istituto Nanoscienze-CNR, Piazza San Silvestro 12, I-56127 Pisa, Italy*

(Received 31 October 2016; accepted 27 December 2016; published online 27 February 2017)

As building blocks of microscopically non-homogeneous materials, semiconductor nanowires and polymer nanofibers are emerging component materials for disordered photonics, with unique properties of light emission and scattering. Effects found in assemblies of nanowires and nanofibers include broadband reflection, significant localization of light, strong and collective multiple scattering, enhanced absorption of incident photons, synergistic effects with plasmonic particles, and random lasing. We highlight recent related discoveries, with a focus on material aspects. The control of spatial correlations in complex assemblies during deposition, the coupling of modes with efficient transmission channels provided by nanofiber waveguides, and the embedment of random architectures into individually coded nanowires will allow the potential of these photonic materials to be fully exploited, unconventional physics to be highlighted, and next-generation optical devices to be achieved. The prospects opened by this technology include enhanced random lasing and mode-locking, multi-directionally guided coupling to sensors and receivers, and low-cost encrypting miniatures for encoders and labels. [http://dx.doi.org/10.1063/1.4974481]

Disordered photonics is a relatively new branch of optics which studies how microscopically non-homogeneous materials, scattering light waves along random directions, can be utilized to highlight unconventional physics and to build novel devices.[1] The lengthscale of disorder in the material has to be of the order of the wavelength (λ) of light. Systems which can be useful in this respect include clusters of nanoparticles, inorganic semiconductor powders, colloids, polymers, biological tissues, aerosols of microdroplets, and porous glasses.[2–8] Important aspects which affect the behaviour of light in these systems are the elastic character of diffusion and the possibility of interference which is not lost even after multiple scattering events, since the phase of optical wavelets is kept well-defined. In this way, many disordered materials are able to provide coherent feedback for light, which, combined with sufficient optical gain given by stimulated emission from some part of the system, is what is needed for achieving lasing. This has led to demonstrating the so-called random lasers,[9] namely, laser sources built by non-homogeneous materials with optical gain. The active medium providing gain can be either inorganic[2,3] or organic.[5,6] Since an external cavity is missing, random architectures might greatly simplify the realization and reduce the cost of laser devices, especially for applications where low coherence might be desired, such as for speckle-free imaging.[10] Other target fields for random lasers include chemical and biological sensors, and medical diagnostics. For instance, cancerous and healthy tissues are found to show different random lasing spectra once infiltrated with dyes.[11]

Some transport properties of light in these systems can be assessed through coherent backscattering, which highlights constructive interference of waves along momentum-reversed scattering paths,

[a]dario.pisignano@unisalento.it
[b]luana.persano@nano.cnr.it
[c]andrea.camposeo@nano.cnr.it

hence weak localization effects which may occur in the material.[12,13] In general, each photon travelling in the disordered material performs a diffusive random walk assisted by multiple scattering events, similarly to particles in Brownian motion (Fig. 1(a)).[14] Unconventional diffusive behaviours (i.e., superdiffusion), with step lengths during the walk described by a power-law distribution which makes very long steps possible (so-called Lévy flight, Fig. 1(b)), have been also evidenced in engineered, inhomogeneous materials made by glass microspheres and scattering particles with high refractive index (n) embedded in a glass host.[14] Coherent backscattering methods allow the strength of light scattering to be assessed and strongly or weakly scattering materials to be distinguished, by measuring the angle of the cusp which describes the intensity spatial distribution of backscattered light. In this framework, important relationships are those among the involved characteristic length-scales, that is, the mean free photon path (l_S), which is the average distance travelled by photons between consecutive scattering events, and the transport mean free path (l_T), which is the average distance travelled by photons before their path becomes randomized and which can be measured by coherent backscattering. For three-dimensional (3D) diffusing materials, $l_T = l_S/(1 - <\cos\phi>)$, where $<\cos\phi>$ is the averaged cosine of the scattering angles. Measuring the transport mean free

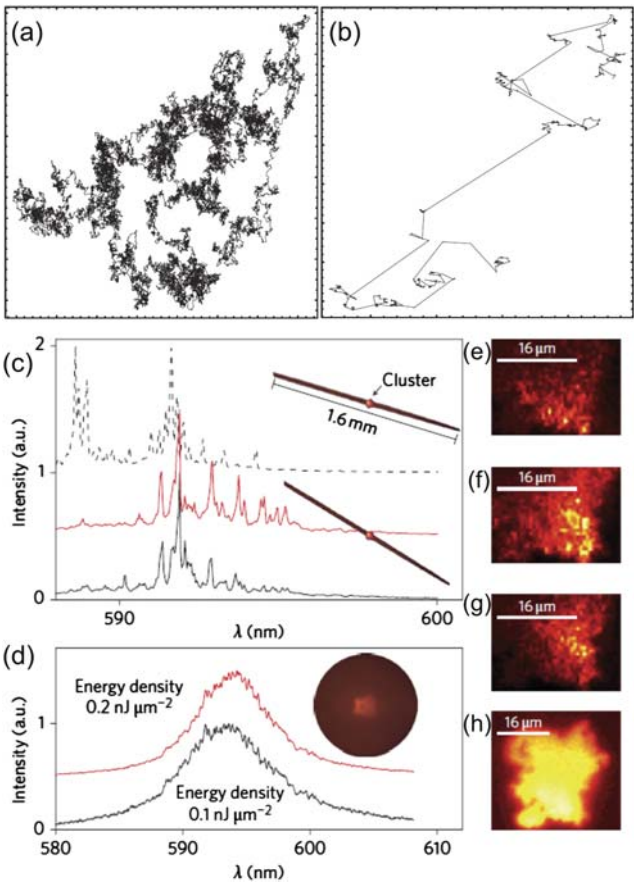

FIG. 1. ((a) and (b)) Exemplary trajectories of random walks for normal Brownian diffusion (a) and for a Lévy flight with higher frequency of long steps. Reprinted with permission from Barthelemy *et al.*, Nature **453**, 495–498 (2008). Copyright 2008 Macmillan Publishers, Ltd. ((c)–(h)) Mode-locking transition in random lasers made of an organic dye solution and nanoparticle clusters. Normalized spectra are shown for samples pumped by a stripe-shaped spot providing directional excitation (c) and by a circular spot (d). Excitation configurations are schematized in the corresponding insets. The three spectra in (c) are collected for various orientations and thicknesses of the excitation stripe. The two spectra in (d) are collected for two different excitation fluences. ((e)–(h)) Random lasing spatial distribution, corresponding to the spectra in (c) (panels (e-g)), and in (d) (panel (h)), respectively. Stripe excitation leads to spatially decoupled modes with hot spots, whereas isotropic excitation leads to correlated modes oscillating together in the emitting region. Reprinted with permission from Leonetti *et al*, Nat. Photonics **5**, 615–617 (2011). Copyright 2011 Macmillan Publishers, Ltd.

path at specific wavelengths allows one to estimate, through the well-known Ioffe-Regel criterion,[9] if weak or strong scattering occurs, i.e., if $kl_T > 1$ (weak scattering) or $kl_T < 1$ (strong scattering), where k is the wavenumber of light ($k = 2\pi/\lambda$). The $kl_T < 1$ condition, which leads to the so-called strong localization or Anderson localization of light,[15,16] namely, to high confinement of light in space, is very hard to fulfill in 3D optical materials. In fact, the spatial extent of optical modes in random photonic systems, especially in random lasers, has been widely debated in the literature.[17–19] More localized states, resulting from constructive interference in the material, would be much less susceptible to couple with other electromagnetic modes and to optical leakages, which would result in a higher quality factor than extended states. On the contrary, when coupling between distant modes occurs, some form of collective optical states can be measured in the system, with a high correlation of the spectra collected from different excited regions which evidences the so-called non-locality.[20] It is generally accepted today that modes with very different spatial extent might coexist in the same complex material undergoing random lasing, depending on local scattering properties as well as pumping fluence, directionality, spot shape, etc (Figs. 1(c)–1(h)).[19,21]

The difficulty in strongly localizing light in three dimensions is one of the reasons which motivates research in disordered photonics to consider materials with reduced dimensionality, where spatial inhomogeneity in the optical media introduces additional confinement and where localization effects are more easily obtained. In this respect, complex materials which incorporate regions with n-contrast, which lead to light confinement in the parts with higher index, are especially interesting in view of merging disordered photonics with light waveguiding in unique devices.

The existence of random, high-n regions with preferential confinement of light, such as dielectric waveguides, has been proposed by Apalkov[22] to rationalize the occurrence of resonant feedback random lasing (producing spectrally very narrow emission peaks).[2] Indeed, spatial variations of the refractive index would result in the formation of random cavities, namely, random resonators in the optical material, which stochastically lead to the generation of resonant modes. A larger correlation radius of the disorder, related to the finite size of the scattering regions, would strongly favour the formation of closed loops with high quality factors. Hence, intentionally embedding components with waveguiding capability into disordered light-emitting materials can lead to systems with enhanced or exotic properties of emission, localization, and transport of light. This can be achieved by means of highly elongated particles, such as nanowires and nanofibers, with n values higher than that in the surrounding medium. Nanowires and nanofibers can be hierarchically organized into complex layers with varying degree of disorder or used as dopants within other matrices to build hybrid materials with tailored light emission or scattering. This perspective paper intends to highlight recent findings in the framework of disordered photonic materials based on complex assemblies of nanowires and nanofibers, and to shadow possible developments where these highly elongated nanostructures can offer added value to fundamental studies and applications.

In the following, by nanowires we will mean crystalline or semicrystalline nanostructures with diameter below 100 nm and high length-to-radius (L/R) ratio (axial ratio). They can be either inorganic or organic, their stiffness is considerable given their crystalline character, and they can be realized by various methods such as epitaxial growth, chemical vapor deposition, colloidal synthesis, and deep reactive ion etching.[23–26] Instead, by nanofibers we will mean mechanically flexible nanostructures, such as polymer filaments, which have a prevalently amorphous structure at nanoscale and might exhibit extremely high L/R values.[27] Light-emitting nanofibers can be produced by self-assembly, casting of polymer solutions, polymerization methods, nanofluidics, synthesis assisted by either hard or soft templates, and electrospinning,[26,28] which is based on the uniaxial elongation of a fluid jet driven by an intense applied electric field.[29–31] A common feature of these materials is that nanowires or nanofibers can be organized in almost two-dimensional (2D) layers and in turn serve as anisotropic, almost one-dimensional waveguiding or scattering elements. The waveguides formed by nanowires and nanofibers are often sub-wavelength, namely, they transport light at optical frequencies along their longitudinal axis, although their transversal size is well below the corresponding wavelength.[32,33]

For single nanofibers, the light-scattering properties can be sketched by considering infinitely long dielectric structures with cylindrical shape, under the Rayleigh-Gans approximation for relatively weak scatterers—as in the organic case—which requires $|n - 1| \ll 1$ and $kR|n - 1| \ll 1$.[34] The

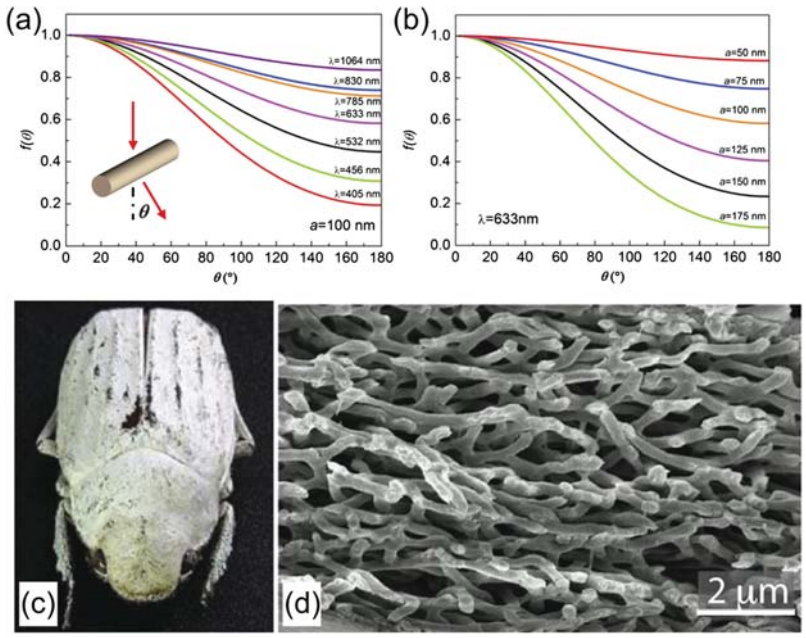

FIG. 2. Organic nanofibers and light-scattering. ((a) and (b)) Angular dependence of the normalized scattering form factor, $f(\theta)$, from a single fiber for different wavelengths (a, fiber radius = 100 nm) and radius values, here a (b, $\lambda = 633$ nm). Inset in (a): scheme of normally incident light and of its diffusion in a plane perpendicular to the fiber axis. Reprinted with permission from Persano *et al.*, Proc. SPIE **9745**, 97450R (2016). Copyright 2016 SPIE. ((c) and (d)) Photograph of a white beetle (*Lepidiota stigma*) (c) and SEM micrograph of chitin rods with angular correlation within a scale (d). The length of individual rods is up to 1 μm. This structure is found to induce very strong out-of-plane scattering and whiteness notwithstanding the high density of fibers. Reprinted with permission from Burresi *et al.*, Sci. Rep. **4**, 6075 (2014). Copyright 2014 Creative Commons CC-BY license.

corresponding form factor, $f(\theta)$, which describes the angular distribution of the scattered intensity, is plotted in Figs. 2(a) and 2(b) for the case of incoming light at normal incidence with respect to the fiber longitudinal axis. The scattering form factor is given by[34,35]

$$f(\theta) = \frac{2J_1[2ka\sin(\theta/2)]}{2ka\sin(\theta/2)}, \tag{1}$$

where θ indicates the polar angle in the plane normal to the fiber length and J_1 is the Bessel function of the first kind with $l = 1$. Light with longer λ or thinner fibers leads to better diffusion at larger angles (Figs. 2(a) and 2(b)).

When multiple scattering effects are scaled to disordered mats of nanowires, the response of the system to incident light becomes more complex, unusual broadband reflection or significant light localization can be achieved, with trapping possibly exceeding limits predicted by ray optics.[36] An insight into the transport properties exhibited by light travelling through random structures made of nanofibers has recently come from the study of the scales of *Cyphochilus* and *Lepidiota stigma* white beetles (Fig. 2(c)).[37] While whiteness is generally produced by ambient light once it is diffused and reflected from relatively thick layers of disordered and strong scatterers, these coleopteras appear white due to very thin scales (thickness ≅ 8–14 μm). To this aim, they have developed dense and anisotropic chitin fibrillar networks, as those displayed in the scanning electron microscopy (SEM) image in Fig. 2(d) which, notwithstanding the quite low refractive index ($n = 1.56$), allow broadband reflection to be obtained. It is known that, when the spatial distribution of scatterers is dense above some threshold packing fraction, namely, when neighbour particles or fibers are very close to each other, the efficiency of light scattering should normally decrease due to the so-called optical crowding. Instead, by means of their fibrillar chitin networks, the scales of white beetles overcome optical crowding and show a transport mean free path as low as 1–2 μm,[37] which is extremely low compared to other organic materials. This is possible because some correlation is present in the angular distribution of fibers, which are prevalently aligned along a direction in the plane. Such specific configuration

leads to anisotropic diffusion of light and to strengthening out-of-plane scattering.[38] It is clear that these biological structures can serve as a model to investigate how the transport of light works in other systems made by anisotropic networks of fibers organized in an almost in-plane configuration, such as epitaxially grown and pressed/partially planarized nanowires and non-woven membranes of electrospun polymer filaments.

In this respect, nanowires made of silicon or other inorganic semiconductors (Fig. 3) are especially interesting in view of improving light trapping in solar cells and allow very high scattering strengths to be obtained upon optimizing the wire dimensions and arrangement.[39–44] Devices based on random Si nanowires have been reported to exhibit a peak external quantum efficiency of about 12%, with an optical reflectance lower by one to two orders of magnitude with respect to planar solar cells.[23] Various other reports have analysed the fundamental aspects of the interaction of light and disordered assemblies of semiconductor nanowires. For instance, fractal structures of Si nanowires fabricated

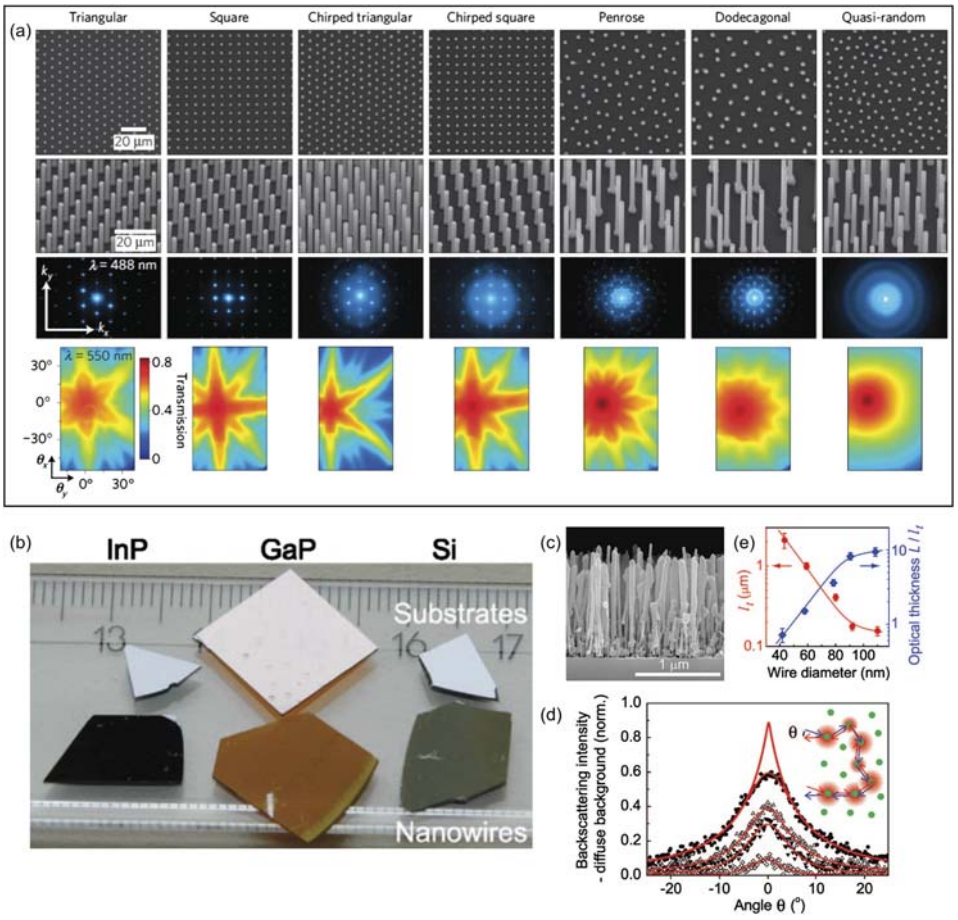

FIG. 3. Inorganic semiconductor nanowires and light-scattering. (a) Examples of patterns of Si nanowires with different degrees of disorder: SEM micrographs (top two rows), corresponding (k_x, k_y) transmitted diffraction patterns for arrays of nanowires embedded in a transparent polymer (third row, $\lambda = 488$ nm), and integrated transmission maps (fourth row, $\lambda = 550$ nm) as a function of the beam incidence angle (θ_x, θ_y). Reprinted with permission from Kelzenberg *et al.*, Nat. Mater. **9**, 239–244 (2010). Copyright 2010 Macmillan Publishers, Ltd. (b) Photograph of samples with deposited InP, GaP, and Si nanowires (bottom row), together with the corresponding pristine substrates (top row). Reprinted with permission from Muskens *et al.*, Nano Lett. **8**, 2638–2642 (2008). Copyright 2008 American Chemical Society. (c) SEM micrograph of GaP nanowires. (d) Corresponding cones of enhanced backscattering ($\lambda = 632$ nm), for wires with different average diameter (from bottom to top: 43, 59, 81, and 110 nm, respectively). Lines superimposed to experimental data are fits by a finite slab model. Inset: schematics of reciprocal transport paths in the scattering material. (e) Transport mean free path and optical thickness (L/l_T) vs. wire diameter. Reprinted with permission from Muskens *et al.*, Nano Lett. **9**, 930–934 (2009). Copyright 2009 American Chemical Society.

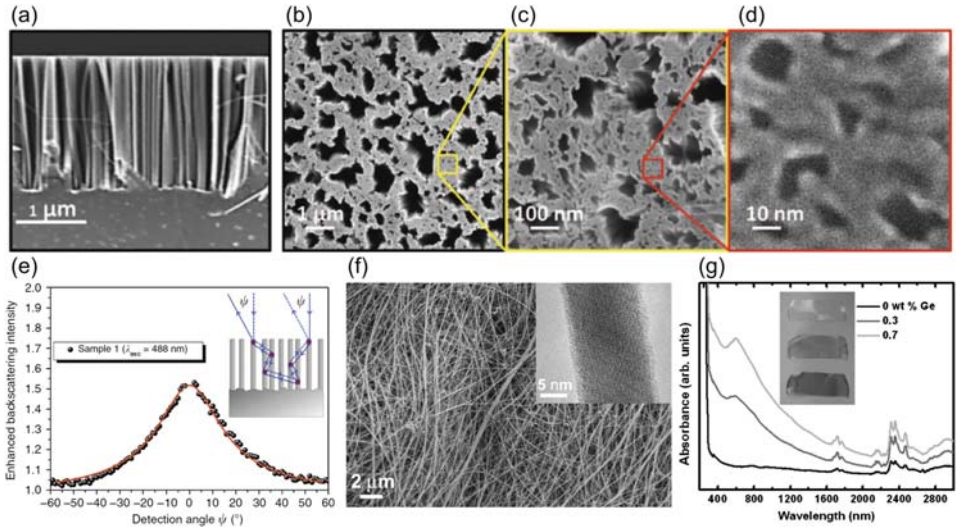

FIG. 4. Light-scattering fractal structures and nanocomposites by semiconductor nanowires. ((a)–(e)) SEM micrographs of vertically grown Si nanowire fractals, with a cross-sectional view (a) and various top views at different magnification ((b)–(d)). (e) Corresponding coherent backscattering cone ($\lambda = 488$ nm) and slab model fit (line superimposed to experimental data). Inset: schematics of reciprocal transport paths in the scattering material. Reprinted with permission from Fazio *et al.*, Light: Sci. Appl. **5**, e16062 (2016). Copyright 2016 Creative Commons CC-BY license. ((f) and (g)) Long Ge nanowires, produced by colloidal synthesis and imaged by SEM (f) and by transmission electron microscopy (TEM, inset in (f)), and corresponding absorbance spectra of composites with different loadings of nanowires (g). Reprinted with permission from Smith *et al.*, J. Phys. Chem. C **114**, 20983–20989 (2010). Copyright 2010 American Chemical Society.

by metal-assisted etching (Figs. 4(a)–4(e)) are found to be very efficient in trapping visible and near-infrared light, and to exhibit enhanced luminescence and Raman scattering.[45] In vertically aligned, disordered forests of nanowires obtained from Si(111) surfaces, fractal dimensions of 1.87 are estimated, and l_T as low as 160 nm is measured by coherent backscattering, which makes this system one of the most strongly scattering materials. Another study, focused on GaP nanowires, has evidenced highly correlated transport of light through pressed mats, with the occurrence of strong and collective effects of multiple scattering.[46] Among possible enabled applications, the activation of nonlinearities is a tool to control destructive and constructive interference in shaped wavefronts by fs-laser excitation.[47] Enhanced absorption[42] is observed as well, even in nanocomposites[41] where nanowires are embedded within polymer matrices (Figs. 4(f) and 4(g)). Layers of crystalline olygophenyl nanowires grown by molecular epitaxy or organic molecular beam deposition as those shown in Fig. 5(a) are another example, utilized to build random lasers.[48–50] Excited by the second harmonic of a Ti:Sapphire regenerative amplifier with 150 fs pulse duration, self-organized layers of *para*-sexiphenyl (*p*-6P) nanowires lase with narrow peaks (Fig. 5(b)) arising from the 0-1 vibronic band of the oligomer (~425 nm), and a threshold as low as 0.5 μJ cm^{-2}.[48] Intensity ratios of 10 dB are measured for the corresponding emission polarization anisotropy, with laser light mostly polarized along the length of nanowires.[50] Single nanowires might also show random lasing, with a threshold fluence below 12 μJ cm^{-2}, based on light scattering and partial reflections along their length due to small cracks or defects.[49]

Flexible mats made by electrospun nanofibers with optical gain can be used to fabricate very cheap lasers in at least two ways. In one approach, randomly distributed resonators made by interconnecting fibers guiding light and forming closed loops produce deterministic lasing, with comb-like emission spectra (Figs. 6(a) and 6(b)).[51] Our group is presently working to realize 3D random lasers based on non-wovens of electrospun polymer nanofibers, produced with either light-emitting, conjugated polymers or plastics doped with lasing dyes (Figs. 6(c) and 6(d)).[52] In recent experiments nanofibers, even of biological origin, have also been combined with metallic nanoparticles to put plasmonic effects in the disordered photonic material into play. For instance, random lasers can be realized, which use flexible membranes made of bacterial cellulose fibrils and Ag nanoparticles.[53] Random

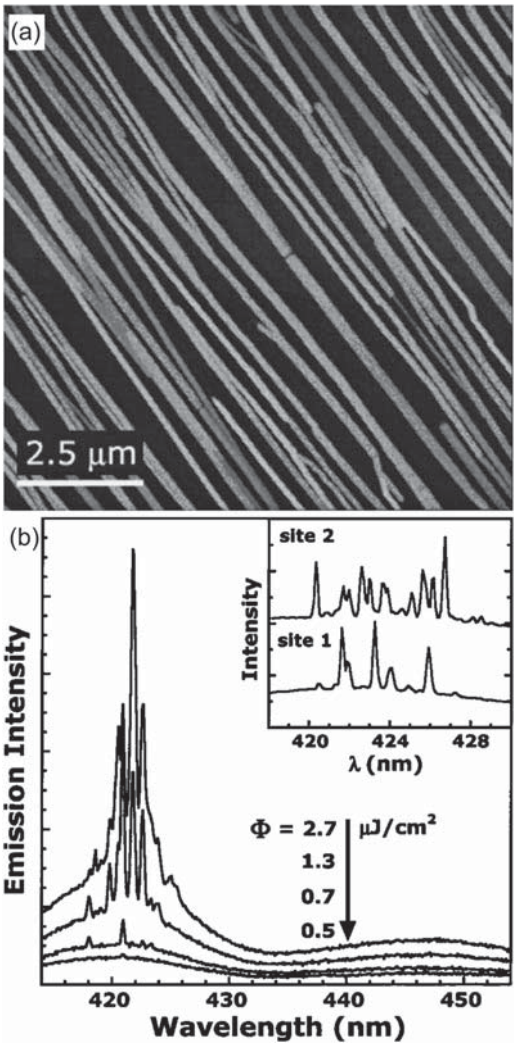

FIG. 5. Random lasing from *p*-6P nanowires. (a) Nanowires grown by hot-wall epitaxy, imaged by atomic force microscopy. Image size $10 \times 10\ \mu m^2$, vertical grayscale 0-220 nm. (b) Room-temperature random lasing emission spectra from nanowires, for various values of the excitation fluence (Φ), at $T = 30$ K. Inset: room-temperature emission spectra from two sample regions. Reprinted with permission from *Quochi et al.*, Appl. Phys. Lett. **84**, 4454–4456 (2004). Copyright 2004 American Institute of Physics.

fiber lasers might exploit plasmonic mechanisms for feedback, which is enabled by doping polymer filaments with metal nanoparticles.[54] Densely packed Ag nanorods in arrays, realized by a glancing angle deposition method and tilted at about 30° with respect to a substrate, induce random lasing in polymer films doped with rhodamine.[55] Forming a plasmonic metamaterial, the nanorods assist the formation of confined laser modes and decrease the lasing threshold up to considerably high packing fraction (7% of metal). Metal nanoparticles can also be directly electrospun together with polymers, thus leading to achieve plasmon-enhanced random lasers.[56] For rhodamine-doped cellulose fibers embedding 10 nm Au nanoparticles, the threshold for lasing is found to decrease by 17% compared to fibers without nanoparticles (Figs. 6(e)–6(h)).

On the base of this set of results, there are many forward-looking aspects inherent in using nanowires and nanofibers in random optical media. While the by far largest number of experiments in the field of amorphous photonics has been performed by spherical, isotropic scattering centers hitherto, important possible developments can be envisaged in the near future exploiting strongly anisotropic semiconductor nanoparticles or organic filaments, which are likely to open new perspectives for nanophotonic devices, such as the following:

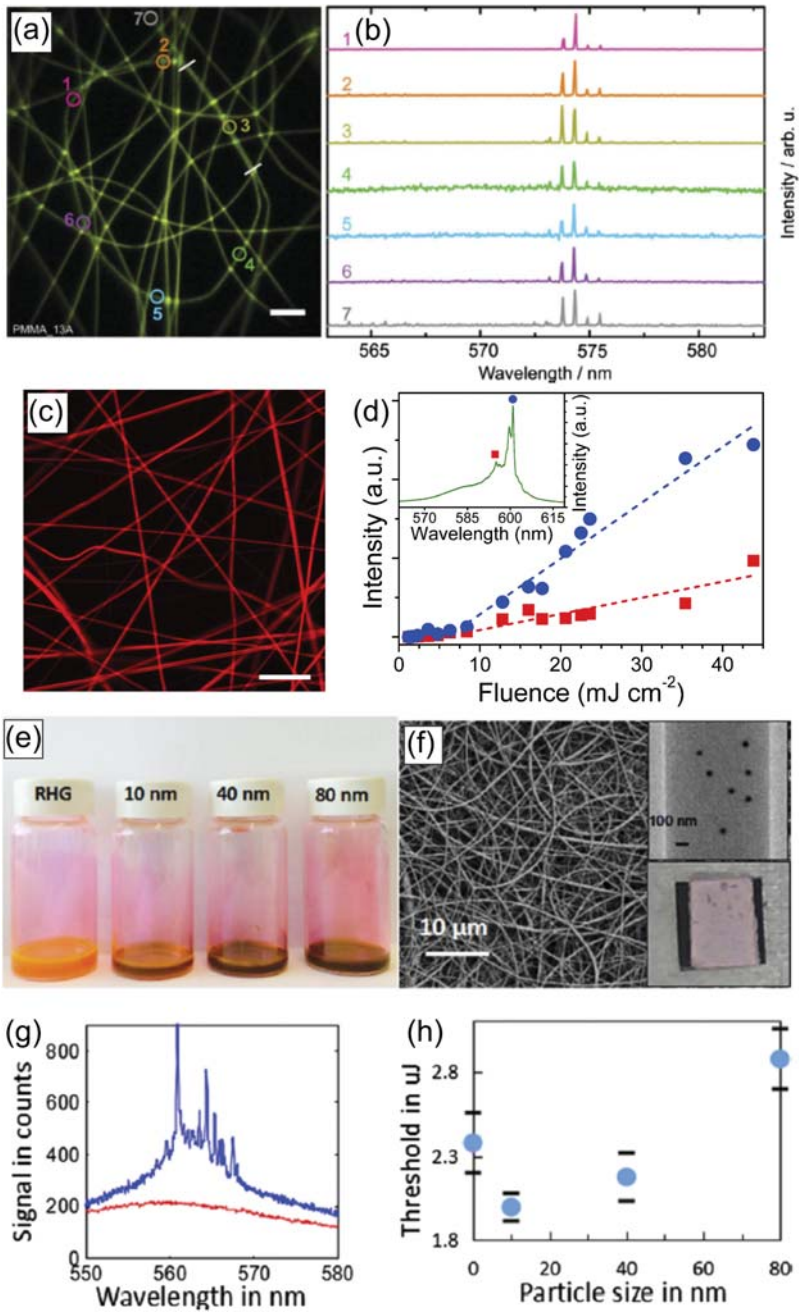

FIG. 6. Electrospun nanofibers as disordered photonic material. ((a) and (b)) Ring resonator, randomly formed by a sub-monolayer coverage through electrospun nanofibers. Circles in (a) indicate different sample positions, whose corresponding lasing spectrum is shown in (b). The white bars in (a) show a region where a contact is established, along a few tens of μm, between the ring resonator and another fiber. Scale bar in (a): 20 μm. Reprinted with permission from Krämmer *et al.*, Adv. Mater. **26**, 8096–8100 (2014). Copyright 2014 WILEY-VCH Verlag GmbH & Co. KGaA. ((c) and (d)) Confocal fluorescence micrograph of randomly oriented, rhodamine-doped nanofibers (scale bar 50 μm) and lasing characteristics (d) and exemplary spectra (inset in (d)) for two modes at about 595 nm (squares) and 601 nm (circles). Reprinted with permission from Persano *et al.*, Proc. SPIE **9745**, 97450R (2016). Copyright 2016 SPIE. ((e)–(h)) Photograph of a rhodamine (RHG) solution and of colloidal Au with different particle size (10, 40, and 80 nm, (e)). (f) Fibers imaged by SEM and by TEM highlighting embedded particles (top inset), and sample image (bottom inset). (g) Emission spectra below (bottom curve) and above (top curve) lasing threshold. (h) Thresholds measured for fibers without particles and for fibers embedding the three types of Au nanoparticles shown in (e). By incorporating 10 nm particles, a significant threshold reduction is measured with respect to all-organic fibers. Reprinted with permission from Zhang *et al.*, Appl. Phys. Lett. **108**, 011103 (2016). Copyright 2016 AIP Publishing, LLC.

(i) Possibility of coupling light modes at different degrees of localization in the complex material with efficient channels for transmission, waveguiding the generated radiation and directing it, possibly multi-directionally, to external sensors or receivers; nowadays, materials conceived to this aim are becoming feasible, which would enhance integration of disordered photonics in device architectures. In addition, strengthening modal interactions can lead to mode-locking in random lasers,[21] which can be critically favoured by waveguiding components such as nanowires and nanofibers embedded in materials. These components may work as additional spectral selectors, favouring guided modes in the competition for lasing, or greatly help to obtain correlated random lasers and to possibly induce enhanced non-locality in the system.

(ii) As previously mentioned, an eventual correlation in the disorder[57] in spatially non-homogeneous materials can significantly affect optical properties. This makes greatly important engineering disorder and controlling correlations.[58] For instance, local correlations in the position of light-scattering particles can be achieved by exploiting electrostatic repulsion in charged colloidal suspensions.[59] This concept can be applied to polymer nanofibers in various ways, in order to tailor correlation and affect the photonic properties of the produced, disordered assembly. Both colloidal processing and electrospinning would in principle allow correlations to be obtained and to some extent controlled. For instance, electrospinning, where fibers are realized by means of electrified jets of polymer solution, is likely to induce correlations in the deposition patterns due to electrostatic interactions as those determining bending instabilities in the jets.[60] Predicting these correlations will allow reliable non-woven structures to be obtained, which would present high extraction efficiency for emitted photons, tailored localization for light in the organic material, or broadband reflection.

(iii) Finally, random architectures can be embedded into individually coded nanowires or nanofibers. Optical necklace states, namely, non-localized modes with very high transmission, could be produced in the resulting, disordered one-dimensional materials.[61] Also, random lasers at single nanowire or nanofiber scale would also serve as highly miniaturized encrypting elements. Technologies to pattern individual light-emitting semiconductor nanowires or polymer nanofibers are already available, such as focused ion beam milling[62] and nanoimprint lithography performed at room temperature,[63] and they can be conveniently addressed to the top-down realization of single-fiber random lasers for encoding and labelling.

We acknowledge the European Research Council for supporting, under the European Union's Seventh Framework Programme (No. FP/2007-2013)/ERC Grant Agreement No. 306357 (ERC Starting Grant "NANO-JETS"). We gratefully thank Dr. M. Moffa, Dr. V. Resta, Dr. V. Fasano, and M. Montinaro for electrospinning fabrication and optical characterization, and Dr. O. M. Maragò, Dr. M. A. Iatì, Professor C. Conti, and Professor J. Myśliwiec for helpful discussion.

[1] D. S. Wiersma, Nat. Photonics **7**, 188 (2013).
[2] H. Cao, Y. G. Zhao, S. T. Ho, E. W. Seelig, Q. H. Wang, and R. P. H. Chang, Phys. Rev. Lett. **82**, 2278–2281 (1999).
[3] D. Anglos, A. Stassinopoulos, R. N. Das, G. Zacharakis, M. Psyllaki, R. Jakubiak, R. A. Vaia, E. P. Giannelis, and S. H. Anastasiadis, J. Opt. Soc. Am. B **21**, 208–213 (2004).
[4] P. D. García, R. Sapienza, Á. Blanco, and C. López, Adv. Mater. **19**, 2597–2602 (2007).
[5] Q. Song, S. Xiao, Z. Xu, J. Liu, X. Sun, V. Drachev, V. M. Shalaev, O. Akkus, and Y. L. Kim, Opt. Lett. **35**, 1425–1427 (2010).
[6] A. Tulek, R. C. Polson, and Z. V. Vardeny, Nat. Phys. **6**, 303–310 (2010).
[7] A. K. Tiwari, R. Uppu, and S. Mujumdar, Opt. Lett. **37**, 1053–1055 (2012).
[8] L. Sznitko, J. Myśliwiec, and A. Miniewicz, J. Polym. Sci., Part B: Polym. Phys. **53**, 951–974 (2015).
[9] D. S. Wiersma, Nat. Phys. **4**, 359–367 (2008).
[10] B. Redding, M. A. Choma, and H. Cao, Nat. Photonics **6**, 355–359 (2012).
[11] R. C. Polson and Z. V. Vardeny, Appl. Phys. Lett. **85**, 1289–1291 (2004).
[12] M. P. van Albada and A. Lagendijk, Phys. Rev. Lett. **55**, 2692–2695 (1985).
[13] P.-E. Wolf and G. Maret, Phys. Rev. Lett. **55**, 2696–2699 (1985).
[14] P. Barthelemy, J. Bertolotti, and D. S. Wiersma, Nature **453**, 495–498 (2008).
[15] P. W. Anderson, Phys. Rev. **109**, 1492–1505 (1958).
[16] E. Abrahams, P. W. Anderson, D. C. Licciardello, and T. V. Ramakrishnan, Phys. Rev. Lett. **42**, 673–676 (1979).
[17] H. Cao, J. Y. Xu, D. Z. Zhang, S.-H. Chang, S. T. Ho, E. W. Seelig, X. Liu, and R. P. H. Chang, Phys. Rev. Lett. **84**, 5584–5587 (2000).
[18] K. L. van der Molen, R. W. Tjerkstra, A. P. Mosk, and A. Lagendijk, Phys. Rev. Lett. **98**, 143901 (2007).
[19] J. Fallert, R. J. B. Dietz, J. Sartor, D. Schneider, C. Klingshirn, and H. Kalt, Nat. Photonics **3**, 279–282 (2009).

[20] M. Leonetti, C. Conti, and C. Lopez, Light: Sci. Appl. **2**, e88 (2013).
[21] M. Leonetti, C. Conti, and C. Lopez, Nat. Photonics **5**, 615–617 (2011).
[22] V. M. Apalkov, M. E. Raikh, and B. Shapiro, Phys. Rev. Lett. **89**, 016802 (2002).
[23] L. Tsakalakos, J. Balch, J. Fronheiser, B. A. Korevaar, O. Sulima, and J. Rand, Appl. Phys. Lett. **91**, 233117 (2007).
[24] E. Garnett and P. Yang, Nano Lett. **10**, 1082–1087 (2010).
[25] N. P. Dasgupta, J. Sun, C. Liu, S. Brittman, S. C. Andrews, J. Lim, H. Gao, R. Yan, and P. Yang, Adv. Mater. **26**, 2137–2184 (2014).
[26] Y. Xia, P. Yang, Y. Sun, Y. Wu, B. Mayers, B. Gates, Y. Yin, F. Kin, and H. Yan, Adv. Mater. **15**, 353–389 (2003).
[27] Given the general higher variability in nanofabrication methods on organics, the size condition ($2R \leq 100$ nm) is frequently relaxed in the literature dealing with polymer nanofibers.
[28] D. Pisignano, *Polymer Nanofibers* (Royal Society of Chemistry, Cambridge, 2013).
[29] D. H. Reneker and I. Chun, Nanotechnology **7**, 216–223 (1996).
[30] D. Li and Y. Xia, Adv. Mater. **16**, 1151–1170 (2004).
[31] A. Camposeo, L. Persano, and D. Pisignano, Macromol. Mater. Eng. **298**, 487–503 (2013).
[32] D. O'Carroll, I. Lieberwirth, and G. Redmond, Nat. Nanotechnol. **2**, 180–184 (2007).
[33] V. Fasano, A. Polini, G. Morello, M. Moffa, A. Camposeo, and D. Pisignano, Macromolecules **46**, 5935–5942 (2013).
[34] L. Persano, M. Moffa, V. Fasano, M. Montinaro, G. Morello, V. Resta, D. Spadaro, P. G. Gucciardi, O. M. Maragò, A. Camposeo, and D. Pisignano, Proc. SPIE **9745**, 97450R (2016).
[35] P. H. Jones, O. M. Maragò, and G. Volpe, *Optical Tweezers: Principles and Applications* (Cambridge University Press, Cambridge, 2015).
[36] D. M. Callahan, J. N. Munday, and H. A. Atwater, Nano Lett. **12**, 214–218 (2012).
[37] M. Burresi, L. Cortese, L. Pattelli, M. Kolle, P. Vukusic, D. S. Wiersma, U. Steiner, and S. Vignolini, Sci. Rep. **4**, 6075 (2014).
[38] L. Cortese, L. Pattelli, F. Utel, S. Vignolini, M. Burresi, and D. S. Wiersma, Adv. Opt. Mater. **3**, 1337–1341 (2015).
[39] O. L. Muskens, J. Gómez Rivas, R. E. Algra, E. P. A. M. Bakkers, and A. Lagendijk, Nano Lett. **8**, 2638–2642 (2008).
[40] O. L. Muskens, S. L. Diedenhofen, B. C. Kaas, R. E. Algra, E. P. A. M. Bakkers, J. Gómez Rivas, and A. Lagendijk, Nano Lett. **9**, 930–934 (2009).
[41] D. A. Smith, V. C. Holmberg, M. R. Rasch, and B. A. Korgel, J. Phys. Chem. C **114**, 20983–20989 (2010).
[42] M. D. Kelzenberg, S. W. Boettcher, J. A. Petykiewicz, D. B. Turner-Evans, M. C. Putnam, E. L. Warren, J. M. Spurgeon, R. M. Briggs, N. S. Lewis, and H. A. Atwater, Nat. Mater. **9**, 239–244 (2010).
[43] S. L. Diedenhofen, O. T. A. Janssen, G. Grzela, E. P. A. M. Bakkers, and J. Gómez Rivas, ACS Nano **5**, 2316–2323 (2011).
[44] V. C. Holmberg, T. D. Bogart, A. M. Chockla, C. M. Hessel, and B. A. Korgel, J. Phys. Chem. C **116**, 22486–22491 (2012).
[45] B. Fazio, P. Artoni, M. A. Iatì, C. D'Andrea, M. J. Lo Faro, S. Del Sorbo, S. Pirotta, P. G. Gucciardi, P. Musumeci, C. S. Vasi, R. Saija, M. Galli, F. Priolo, and A. Irrera, Light: Sci. Appl. **5**, e16062 (2016).
[46] T. Strudley, T. Zehender, C. Blejean, E. P. A. M. Bakkers, and O. L. Muskens, Nat. Photonics **7**, 413–418 (2013).
[47] T. Strudley, R. Bruck, B. Mills, and O. L. Muskens, Light: Sci. Appl. **3**, e207 (2014).
[48] F. Quochi, F. Cordella, R. Orrù, J. E. Communal, P. Verzeroli, A. Mura, G. Bongiovanni, A. Andreev, H. Sitter, and N. S. Sariciftci, Appl. Phys. Lett. **84**, 4454–4456 (2004).
[49] F. Quochi, F. Cordella, A. Mura, G. Bongiovanni, F. Balzer, and H.-G. Rubahn, J. Phys. Chem. B **109**, 21690–21693 (2005).
[50] F. Quochi, J. Opt. **12**, 024003 (2010).
[51] S. Krämmer, C. Vannahme, C. L. C. Smith, T. Grossmann, M. Jenne, S. Schierle, L. Jørgensen, I. S. Chronakis, A. Kristensen, and H. Kalt, Adv. Mater. **26**, 8096–8100 (2014).
[52] See www.nanojets.eu for detailed information about produced nanofiber materials.
[53] M. V. dos Santos, C. T. Dominguez, J. V. Schiavon, H. S. Barud, L. S. A. de Melo, S. J. L. Ribeiro, A. S. L. Gomes, and C. B. de Araújo, J. Appl. Phys. **115**, 083108 (2014).
[54] S. Li, L. Wang, T. Zhai, L. Chen, M. Wang, Y. Wang, F. Tong, Y. Wang, and X. Zhang, Opt. Express **24**, 12748 (2016).
[55] Z. Wang, X. Meng, S. H. Choi, S. Knitter, Y. L. Kim, H. Cao, V. M. Shalaev, and A. Boltasseva, Nano Lett. **16**, 2471–2477 (2016).
[56] R. Zhang, S. Knitter, S. F. Liew, F. G. Omenetto, B. M. Reinhard, H. Cao, and L. Dal Negro, Appl. Phys. Lett. **108**, 011103 (2016).
[57] G. M. Conley, M. Burresi, F. Pratesi, K. Vynck, and D. S. Wiersma, Phys. Rev. Lett. **112**, 143901 (2014).
[58] K. Vynck, M. Burresi, F. Riboli, and D. S. Wiersma, Nat. Mater. **11**, 1017–1022 (2012).
[59] L. F. Rojas-Ochoa, J. M. Mendez-Alcaraz, J. J. Sáenz, P. Schurtenberger, and F. Scheffold, Phys. Rev. Lett. **93**, 073903 (2004).
[60] D. H. Reneker, A. L. Yarin, H. Fong, and S. Koombhongse, J. Appl. Phys. **87**, 4531–4547 (2000).
[61] J. Bertolotti, S. Gottardo, D. S. Wiersma, M. Ghulinyan, and L. Pavesi, Phys. Rev. Lett. **94**, 113903 (2005).
[62] A. Fu, H. Gao, P. Petrov, and P. Yang, Nano Lett. **15**, 6909–6913 (2015).
[63] L. Persano, A. Camposeo, P. Del Carro, V. Fasano, M. Moffa, R. Manco, S. D'Agostino, and D. Pisignano, Adv. Mater. **26**, 6542–6547 (2014).